JCTC Journal of Chemical Theory and Computation

pubs.acs.org/JCTC Letter

Parallel Implementation of the Density Matrix Renormalization Group Method Achieving a Quarter petaFLOPS Performance on a Single DGX-H100 GPU Node

Andor Menczer, Maarten van Damme, Alan Rask, Lee Huntington, Jeff Hammond,* Sotiris S. Xantheas,* Martin Ganahl,* and Örs Legeza*

Cite This: J. Chem. Theory Comput. 2024, 20, 8397−8404

ABSTRACT: We report cutting edge performance results on a single node hybrid CPU-multi-GPU implementation of the spin adapted *ab initio* Density Matrix Renormalization Group (DMRG) method on current state-of-the-art NVIDIA DGX-H100 architectures. We evaluate the performance of the DMRG electronic structure calculations for the active compounds of the FeMoco, the primary cofactor of nitrogenase, and cytochrome P450 (CYP) enzymes with complete active space (CAS) sizes of up to 113 electrons in 76 orbitals [CAS(113, 76)] and 63 electrons in 58 orbitals [CAS(63, 58)], respectively. We achieve 246 teraFLOPS of sustained performance, an improvement of more than 2.5× compared to the performance achieved on the DGX-A100 architectures and an 80× acceleration compared to an OpenMP parallelized implementation on a 128-core CPU architecture. Our work highlights the ability of tensor network algorithms to efficiently utilize high-performance multi-GPU hardware and shows that the combination of tensor networks with modern large-scale GPU accelerators can pave the way toward solving some of the most challenging problems in quantum chemistry and beyond.

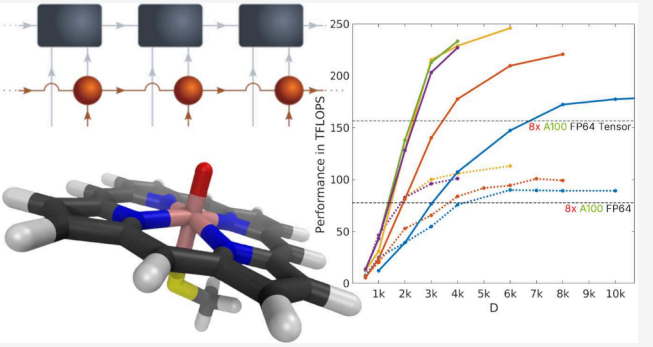

INTRODUCTION

Our current understanding of the properties of molecules and materials rests on the foundations of quantum mechanics. Many modern technologies—such as semiconductor devices,[1] magnetic resonance imaging (MRI), nuclear power or photovoltaic cells—would be impossible without the fundamental understanding of the underlying quantum mechanical effects governing the processes that are responsible for the development of these technologies. The properties of any molecule or material can in theory be computed from solutions of the Schrödinger equation, but obtaining the exact solution is in general impossible except in rare special cases,[2] leaving scientists with the need to settle for approximations. The exponential growth in computational power over the last few decades has led to approximate numerical methods that have become the predominant choice for modeling materials and molecules in both scientific and industrial applications. Prominent examples include density functional theory (DFT)[3−6] (which has become a standard tool in the scientific community and beyond[7−19]), single and multireference Coupled Cluster (CC)[20−26] approaches, quantum Monte Carlo (QMC)[27−33] and various other approximations of full configuration interaction (FCI),[34−45] or tensor networks,[46−62] to name a few. Despite the tremendous algorithmic and hardware advances over the last half century, many quantum mechanical phenomena in chemistry, material science, and condensed matter physics are still not thoroughly understood. Examples include the mechanism of action of biological enzymes,[63−73] the properties of exotic phases of matter[74−76] (including the debated existence of anyonic quasi-particles[77,78]), or even the exact mechanisms of observed cases of high-temperature superconductivity in certain materials.[79−81] A common theme among these phenomena is that they all require the solutions of the many-body Schrödinger equation to obtain a proper understanding of their electronic structure in their ground and excited electronic states. In this context, tensor networks have emerged as one of the most powerful numerical approaches for tackling these challenging problems.[49,75,82−85] Tensor networks are a class of many-body wave functions that can be efficiently stored and manipulated

Received: July 11, 2024
Revised: September 4, 2024
Accepted: September 5, 2024
Published: September 19, 2024

https://doi.org/10.1021/acs.jctc.4c00903
J. Chem. Theory Comput. 2024, 20, 8397−8404

using classical hardware. Tensor networks can parametrize wave functions obeying an area law of entanglement[86] with possibly logarithmic corrections,[84,87] and can be combined with local unitary optimization to reduce entanglement.[88−90] They are also ideally suited to parametrize ground states of gapped, local quantum systems in 1d and 2d. The most successful tensor network, the matrix product state (MPS), is arguably the gold standard approach for obtaining ground states of strongly correlated quantum systems in 1d and 2d.[75] In the area of quantum chemistry, the density matrix renormalization group (DMRG) algorithm, a variational optimization algorithm over the space of MPS, has emerged at the forefront of strongly correlated electron methods, and is widely regarded as a gold standard method for systems encompassing multireference character.[53,55,56,58,59,62,88,91−93] The core operations required in the vast majority of all tensor network algorithms are tensor contraction and matrix factorization, both of which are highly amenable to parallelization and Graphics Processing Unit (GPU) acceleration.[90,94−106] In this context, growing attention is being focused toward developing novel tensor network algorithms that can efficiently utilize highly specialized Artificial Intelligence (AI) accelerators. Examples include recent work on $SU(2)$ spin adapted implementations of DMRG run on NVIDIA DGX-A100[107] architectures,[90,104,105] or multinode multi-GPU architectures.[106,108]

In this work we report on recent progress using large-scale multi-GPU hardware to substantially accelerate tensor network simulations for quantum chemistry and materials science applications. Benchmark calculations of our highly parallelized, GPU-accelerated and SU(2)-aware implementation of the DMRG algorithm on NVIDIA DGX-H100 GPU supercomputers have achieved sustained performance of ∼250 teraFLOPS (trillion floating-point calculations per second) which represents an 80× speedup compared to a state-of-the-art implementation on a traditional Central Processing Unit (CPU) executed on a 128-core CPU architecture.

NUMERICAL PROCEDURE

In the following we will discuss performance benchmarks for the DMRG method for quantum chemistry applications. The DMRG algorithm is the oldest and most important tensor network algorithm, and can be understood as a variational method in the space of so-called matrix product state (MPS)[109] wave functions. In the quantum chemistry context, an MPS is a parametrization of a many-body wave function in terms of N spinful orbitals $|i_n\rangle$ using N order-3 tensors $A^{i_n}_{\alpha_{n-1}\alpha_n}$ of dimension $(D_{n-1}, 4, D_n)$; i.e.,

$$|\Psi_{MPS}\rangle = \sum_{\{i_k\}} \sum_{\{\alpha_p\}} [A_1]^{i_1}_{1\alpha_1} [A_2]^{i_2}_{\alpha_1\alpha_2} \ldots [A_N]^{i_N}_{\alpha_{N-1}1} |i_1 \ldots i_k\rangle \tag{1}$$

where the first and the last are order-2 tensors or matrices. The DMRG algorithm can be used to construct a variational approximation to the ground state of the quantum chemistry Hamiltonian H over the space of MPS; i.e.,

$$E_{opt} = \min_{|\Psi_{MPS}\rangle} \frac{\langle \Psi_{MPS}|H|\Psi_{MPS}\rangle}{\langle \Psi_{MPS}|\Psi_{MPS}\rangle} \tag{2}$$

The bond dimension $D \equiv \max(\{D_n\})$ controls the accuracy of the approximation (larger D is better), with values of $D \sim O(10^4)$ often mandatory to reach sufficient accuracy in quantum chemistry applications. The computational complexity and memory requirements of DMRG scale as $O(D^3N^4)$ and $O(D^2N^2)$, respectively. The DMRG algorithm performs an iterative optimization (one MPS tensor update at a time) of the wave function, where each update is obtained by solving a large hermitian eigenvalue problem using, e.g., the Lanczos or Davidson method. This step usually accounts for 80% of the execution time, and scales as $O(D^3)$. One sequence of updates of all tensors is called a DMRG sweep. For more details on the DMRG and tensor networks in general, we refer the reader to the existing literature.[54,57,59,62,110−114]

PERFORMANCE ASSESSMENT

In the following we present performance benchmarks of DMRG-CAS(M, N) of M electrons in N active orbitals on DGX-H100[115] for a series of increasingly complex molecular systems, namely F_2 [CAS(18, 18)],[83] N_2 [CAS(14, 28)],[116] the Iron-Molybdenium cofactor [FeMoco, CAS(54, 54)][117] and CAS(113, 76),[118] and the activated heme group of cytochrome P450 [CAS(63, 58).[65] Here, we solely rely on implementations previously introduced in refs[104,105] All bond dimensions D are reported as SU(2) multiplets, with the corresponding U(1) bond dimensions indicated separately where applicable.

In Figure 1 we show the performance results of our DMRG implementation on the above-mentioned systems, and for increasing values of SU(2) bond dimension D. For all

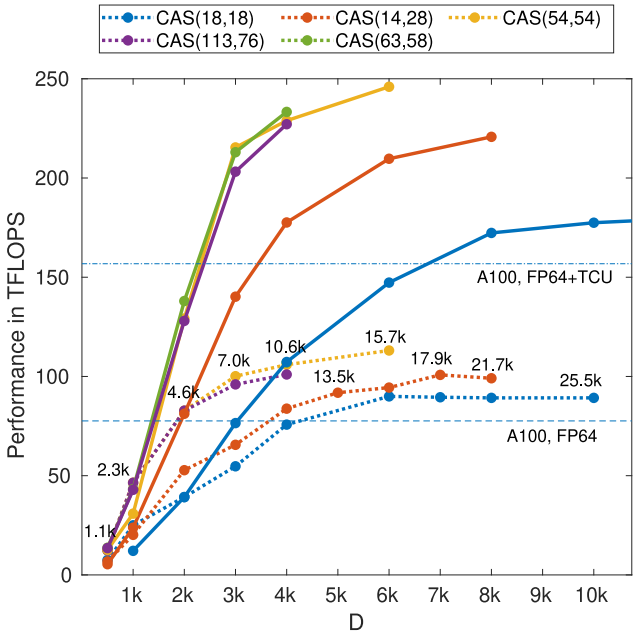

Figure 1. Benchmark results obtained via the SU(2) spin-adapted single node hybrid CPU plus multi-GPU DMRG calculations for the F_2 molecule on a CAS(18,18) orbital space,[83] the N_2 molecule on a CAS(14,28) space,[116] FeMoco on CAS(54,54)[117] and CAS-(113,76)[118] spaces, and P450 on CAS(63,58).[65] The solid lines correspond to calculations performed on a DGX-H100 system. As a reference, the dotted lines trace the results obtained on a DGX-A100 system. The estimated FP64 theoretical upper bound for DGX-A100 is shown by the horizontal dashed line, while the same but also including specialized tensor core units (TCUs) by the horizontal dashed−dotted line. Numbers indicate the corresponding $U(1)$ bond dimension values, which are the same for both the dotted and the solid lines.

https://doi.org/10.1021/acs.jctc.4c00903
J. Chem. Theory Comput. 2024, 20, 8397−8404

simulations we observe an initial linear increase in performance with increasing D and a problem-dependent saturation value. For the smallest systems [CAS(18,18)], the performance saturates at ∼180 teraFLOPS. For the largest systems [CAS(54,54) and CAS(63, 58)] we achieve sustained performance of ∼250 teraFLOPS and expect to reach the performance plateau between $D \approx 8000-10000$. Beyond these bond dimensions, host-device data communication[119] starts to become the dominating factor due to memory limitations on the DGX-H100 and causes a performance breakdown for these large CAS DMRG simulations. However, we expect that MPI-based approaches[106,108] and advanced hardware (such as GH200[120] or AMD MI300[121] superchips) will mitigate this problem and allow us to scale simulations well into and eventually surpassing this regime. Indeed, for GH200 and MI300 hardware, the CPU and GPU have direct shared-memory access across the node, largely eliminating the host-device communication bottleneck. For a more detailed discussion on the nature of the CAS-size dependence of the performance plateau values, we refer the reader to ref.[104]

In summary, we observe an almost ideal 2.5× increase in performance compared to DGX-A100 (dashed lines in Figure 1) and an 80× increase compared to other state-of-the-art OpenMP parallelized implementations of quantum-chemistry DMRG calculations on 128 CPU cores.[104] Two key hardware features that allow us to achieve such performance gains are the massive compute throughput and high memory bandwidth on DGX-H100, as well as the availability of efficient implementations of core linear algebra subroutines in NVIDIA math libraries (CUBLAS).

In Figure 2 we show the total wall time spent in the Davidson diagonalization (including host-device communication) over seven DMRG sweeps as a function of bond dimension D for the systems considered above. Consistent with Figure 1, we observe a linear increase in the wall time for bond dimensions below the performance plateau, and the expected D^3 scaling once we reach the performance plateau.

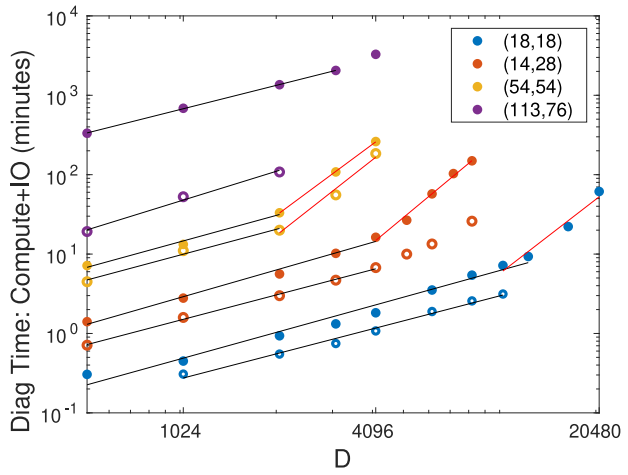

Figure 2. Total diagonalization time of seven DMRG sweeps for the eight GPU accelerated diagonalization procedure measured in minutes including host-device IO overhead for the F_2 CAS(18,18), N_2 CAS(14,28), FeMoco CAS(54,54), and CAS(113,76) as a function of DMRG bond dimension on A100 (solid dot symbol, ●) and on H100 (open symbol, ○) architectures. The solid lines are results of first-order polynomial fits on selected data sets corresponding to measured performance up to saturation of GPU performance (black) and for a region where performance is saturated (red). The fitted exponents for the H100 calculations are 1.05 ± 0.1 and 2.95 ± 0.2, respectively.

Due to the high performance of the latest generations of GPUs and the high degree of parallelization of our DMRG implementation, the wall time for the diagonalization step is reduced to a point where it is no longer the limiting operation, and instead data transfer operations between CPU memory and storage media become the bottleneck. We utilize data compression techniques and asynchronous data transfer approaches to partially mitigate this problem, at the cost of increasing memory requirements by ∼30%. For multinode systems, distributed data approaches[99,103,106,108] can be used to mitigate similar data transfer bottlenecks. For further details on how the different DMRG components contribute to the total wall time in a given iteration step we guide readers to ref,[90] where a more precise performance analysis of the Davidson diagonalization method is also presented.

SPIN STATES OF CYTOCHROME P450 HEME GROUP

In the following we present DMRG-CAS results for the low-lying spin states of the heme-group of the Cytochrome P450 (3A4 isoform) enzyme in its active state (Cpd I).[65] Cytochromes are heme-containing enzymes primarily responsible for detoxification of organisms,[65,122,123] where the heme-group, an iron porphyrin system, is responsible for catalyzing chemical reactions with substrates of the enzyme. Iron porphyrin structures appear as key building blocks in various enzymes. In the active state of P450 (3A4), the iron-porphyrin ring has an oxygen and cysteine bound to the central Fe atom above and below the iron-coordinating plane. Their low-lying energy spectrum features three nearly degenerate states with spin $s = 1/2$, 3/2 ,and 5/2, whose relative energies depend on the geometry and the local chemical environment of the heme group. A full understanding of the electronic structure of this system remains an open problem.[66−73,124] The multireference character and the near-degeneracy of the doublet ($s = 1/2$) and quartet ($s = 3/2$) states[66] pose significant challenges for existing computational approaches, with large active spaces being crucial for obtaining qualitatively and quantitatively accurate results.[66,71] Here, we revisit the problem of computing the DMRG energies of the $s = 1/2$, 3/2, and 5/2 states for the active spaces defined in,[65] and extend them to the CAS(63, 58) space. To the best of our knowledge, this is the largest DMRG-CAS calculation reported to date for this compound. Our primary aim is to demonstrate the ability of our SU(2) symmetric, GPU-accelerated DMRG implementation to perform high accuracy calculations on very large active spaces with large bond dimension within a significantly reduced runtime on DGX-H100 machines.

In Figure 3 we present the $1/D$ scaling analysis of the calculated energies using 13 DMRG sweeps for the lowest lying eigenstates with total spin 1/2 (left panel), 3/2 (middle panel), and 5/2 (right panel) used to obtain the truncation free extrapolated $D \to \infty$ limit[54] for the different CAS spaces (solid lines are second order polynomial fits). The extrapolated energies for the spin 1/2−3/2 and 1/2−5/2 gaps are shown for increasing CAS space sizes in Figure 4. We observe a degeneracy on the order of 0.1 mHartree for the doublet and quartet states, which lies within the established accuracy of the largest measured DMRG truncation error (order 10^{-2} mHartree for $D \leq 4096$). The spin 1/2−5/2 gap (right

https://doi.org/10.1021/acs.jctc.4c00903
J. Chem. Theory Comput. 2024, 20, 8397−8404

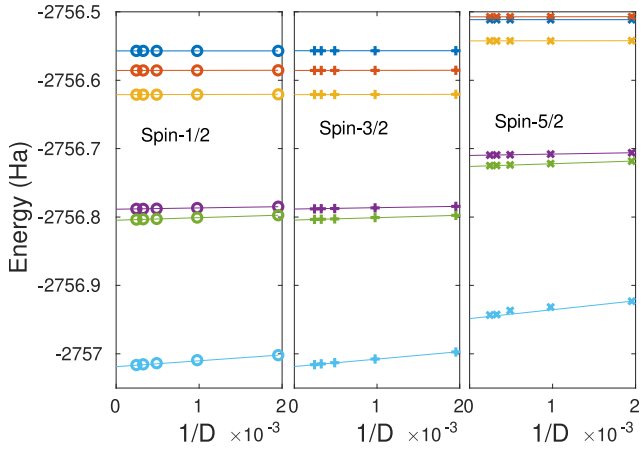

Figure 3. Scaling of the energy for spin states with total spin 1/2 (left panel), 3/2 (middle panel), and 5/2 (right panel) as a function of the inverse DMRG SU(2) bond dimension for the Cytochrome P450 enzyme for the model spaces of CAS(17,15), CAS(25,23), CAS(33,31), CAS(45,41), CAS(47,43), and CAS(63,58) introduced in ref 65, shown by dark blue, red, orange, purple, green, and light blue colors, respectively. Solid lines are the result of second-order polynomial fits.

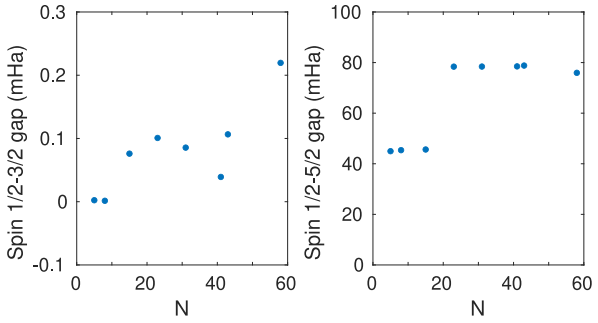

Figure 4. Extrapolated ($D \rightarrow \infty$) spin gap (mHartree) between the spin 1/2 ground and spin 3/2 excited states (left panel) and between the spin 1/2 ground and spin 5/2 excited states (right panel) as a function of model CAS spaces with increasing complexity, i.e., with increasing number of orbitals and number of electrons (data from ref 65).

panel of Figure 4) remains positive and the spin 5/2 state lies above both the spin 1/2 and spin 3/2 states. To provide further insights regarding convergence and computational complexity, the change between the energies of the last two DMRG sweeps was less than 10^{-5} and for D = 4k the corresponding $D_{U(1)}$ bond dimension was found to be 15.6k, 22.3k, and 29.1k, for the 1/2, 3/2, and 5/2 states, respectively. Therefore, in our calculations the largest $U(1)$ bond dimension was twice as large compared to the one used in ref 106, albeit at a significantly reduced runtime and memory costs.

However, in order to resolve the spin gaps at a high level of accuracy (or even capture the qualitative behavior) it is imperative to extend the calculations to larger active spaces while including dynamical correlation effects (e.g., via NEVPT2, the tailored coupled cluster (TCC)[125] or the restricted active space DMRG-RAS-X[126,127] methods). Namely, the resolution of the spin gaps is highly dependent upon a balanced treatment of static and dynamic correlation effects for all three spin states. We have also performed DMRG-CASSCF[128] calculations on this system, using smaller active spaces, which yield substantially lower energies compared to calculations with fixed nonoptimized orbitals. This is part of currently ongoing research and will be published in the near future.

We emphasize again that the high performance of our DMRG implementation, in particular observed already at small bond dimensions, yields substantial accelerations by almost 2 orders of magnitude, allowing calculations for CAS sizes far beyond the current computational limits already feasible on single-node GPU accelerators. We expect future advances enabling DMRG calculations based on CAS spaces well beyond CAS(100,100) will soon be possible on multinode, multi-GPU hardware architectures.[106,108]

CONCLUSIONS AND OUTLOOK

In this work we report state-of-the-art performance results obtained on a single node NVIDIA DGX-H100 architecture via the spin adapted *ab initio* density matrix renormalization group method. We observe a 2.5× speedup compared to a DGX-A100 node or equivalently an 80× speedup compared to an OpenMP parallelized 128 core CPU implementation. These performance improvements reduce run times of typical DMRG calculations for quantum chemistry applications from many days to a few hours, making it possible to potentially apply DMRG routinely in scientific and industrial applications. We expect that with the development of even more advanced classical hardware in the near future, and their extension to shared-memory, multinode multi-GPU architectures, tensor network calculations well beyond CAS(100,100) to be achievable within hours. Such large CAS calculations may help elucidate the electronic mechanisms behind some of the most elusive chemical systems, such as multireference transition metal systems, catalysts, or metalloenzymes. We want to emphasize that a truly quantitatively correct description of such challenging problems requires a careful selection of the orbital active space and a balanced treatment of static and dynamic correlation effects. Chemists today largely rely on their intuition to find appropriate active spaces, and the question of finding the right one for a given system is a currently unsolved problem.[129−131] The ability to quickly iterate on different choices of large active spaces enables a more systematic search for an appropriate active space description. Combined with the ability to perform CASSCF calculations on larger active spaces in similarly short times, and robust approaches for CAS selection,[129−131] represents a significant step forward toward solving the CAS selection problem and obtaining quantitatively and qualitatively unambiguous results for strongly correlated systems.

Tensor network algorithms like DMRG,[132] projected entangled pair states (PEPS),[85] or the multiscale entanglement renormalization ansatz (MERA)[84] occupy a space at the intersection of classical and quantum computing, and are considered to be among the most powerful classical methods to treat strongly correlated and weakly entangled quantum systems. They play a key role in the quest for achieving quantum advantage, both for providing the best known classical answers to reference for many challenging problems[65,133−138] and as fundamental tools for building and testing quantum algorithms,[139,140] simulating and understanding the real-time behavior of quantum hardware,[141−144] and performing error correction.[145] GPU accelerated tensor network algorithms can be expected to have significant impact in these areas in the years to come, and we expect our results to further boost community efforts aimed at the stand-

https://doi.org/10.1021/acs.jctc.4c00903
J. Chem. Theory Comput. 2024, 20, 8397−8404

ardization and adoption of large-scale, GPU accelerated tensor contraction methods and libraries.[146]

AUTHOR INFORMATION

Corresponding Authors

Jeff Hammond − *NVIDIA Helsinki Oy, 00180 Helsinki, Finland;* orcid.org/0000-0003-3181-8190; Email: jeffpapers@nvidia.com

Sotiris S. Xantheas − *Advanced Computing, Mathematics, and Data Division, Pacific Northwest National Laboratory, Washington 99354, United States; Department of Chemistry, University of Washington, Seattle, Washington 98195, United States;* orcid.org/0000-0002-6303-1037; Email: Sotiris.Xantheas@pnnl.gov

Martin Ganahl − *SandboxAQ, Palo Alto, California 94301, United States*; Email: martin.ganahl@sandboxaq.com

Örs Legeza − *Strongly Correlated Systems Lendület Research Group, Wigner Research Centre for Physics, H-1525 Budapest, Hungary; Dynaflex Ltd., 1028 Budapest, Hungary; Institute for Advanced Study, Technical University of Munich, Germany, 85748 Garching, Germany; Parmenides Stiftung, 82343 Pöcking, Germany;* orcid.org/0000-0002-9746-5802; Email: legeza.ors@wigner.hu

Authors

Andor Menczer − *Strongly Correlated Systems Lendület Research Group, Wigner Research Centre for Physics, H-1525 Budapest, Hungary; Eötvös Loránd University, 1117 Budapest, Hungary*

Maarten van Damme − *SandboxAQ, Palo Alto, California 94301, United States*

Alan Rask − *SandboxAQ, Palo Alto, California 94301, United States*

Lee Huntington − *SandboxAQ, Palo Alto, California 94301, United States*

Complete contact information is available at: https://pubs.acs.org/10.1021/acs.jctc.4c00903

Notes

The authors declare no competing financial interest.

ACKNOWLEDGMENTS

This work has been supported by the Hungarian National Research, Development and Innovation Office (NKFIH) through Grant Nos. K134983 and TKP2021-NVA-04, by the Quantum Information National Laboratory of Hungary. Ö.L. and S.S.X. acknowledge support from the Center for Scalable and Predictive Methods for Excitation and Correlated Phenomena (SPEC), funded as part of the Computational Chemical Sciences, FWP 70942, by the U.S. Department of Energy (DOE), Office of Science, Office of Basic Energy Sciences, Division of Chemical Sciences, Geosciences, and Biosciences at Pacific Northwest National Laboratory. Ö.L. also acknowledges financial support by the Hans Fischer Senior Fellowship programme funded by the Technical University of Munich—Institute for Advanced Study. The simulations were performed using Google Cloud Service and the Wigner Scientific Computational Laboratory (WSCLAB).

REFERENCES

(1) Bardeen, J.; Brattain, W. H. The Transistor, A Semi-Conductor Triode. *Phys. Rev.* **1948**, *74*, 230−231.

(2) Francesco, P.; Mathieu, P.; Sénéchal, D. *Conformal field theory*; Springer Science & Business Media, 2012.

(3) Kohn, W.; Sham, L. J. Self-Consistent Equations Including Exchange and Correlation Effects. *Phys. Rev.* **1965**, *140*, A1133−A1138.

(4) Cohen, A. J.; Mori-Sánchez, P.; Yang, W. Challenges for Density Functional Theory. *Chem. Rev.* **2012**, *112*, 289−320.

(5) Becke, A. D. Perspective: Fifty years of density-functional theory in chemical physics. *J. Chem. Phys.* **2014**, *140*, 18A301.

(6) Jones, R. O. Density functional theory: Its origins, rise to prominence, and future. *Rev. Mod. Phys.* **2015**, *87*, 897−923.

(7) Neese, F.; Wennmohs, F.; Becker, U.; Riplinger, C. The ORCA quantum chemistry program package. *J. Chem. Phys.* **2020**, *152*, 224108.

(8) Aprà, E. e. a.; et al. NWChem: Past, present, and future. *J. Chem. Phys.* **2020**, *152*, 184102.

(9) Werner, H.-J.; Knowles, P. J.; Knizia, G.; Manby, F. R.; Schütz, M. Molpro: a general-purpose quantum chemistry program package. *WIREs Computational Molecular Science* **2012**, *2*, 242−253.

(10) Frisch, M. J.; et al.*Gaussian 16*, Rev. C.01; Gaussian: Wallingford, CT, 2016.

(11) Shao, Y.; et al. Advances in molecular quantum chemistry contained in the Q-Chem 4 program package. *Mol. Phys.* **2015**, *113*, 184−215.

(12) te Velde, G.; Bickelhaupt, F. M.; Baerends, E. J.; Fonseca Guerra, C.; van Gisbergen, S. J. A.; Snijders, J. G.; Ziegler, T. Chemistry with ADF. *J. Comput. Chem.* **2001**, *22*, 931−967.

(13) Kresse, G.; Hafner, J. *Ab initio* molecular-dynamics simulation of the liquid-metal−amorphous-semiconductor transition in germanium. *Phys. Rev. B* **1994**, *49*, 14251−14269.

(14) Sun, Q.; Berkelbach, T. C.; Blunt, N. S.; Booth, G. H.; Guo, S.; Li, Z.; Liu, J.; McClain, J. D.; Sayfutyarova, E. R.; Sharma, S.; Wouters, S.; Chan, G. K.-L. PySCF: the Python-based simulations of chemistry framework. *WIREs Comput. Mol. Sci.* **2018**, *8*, No. e1340.

(15) Seritan, S.; Bannwarth, C.; Fales, B. S.; Hohenstein, E. G.; Isborn, C. M.; Kokkila-Schumacher, S. I. L.; Li, X.; Liu, F.; Luehr, N.; Snyder, J. W., Jr.; Song, C.; Titov, A. V.; Ufimtsev, I. S.; Wang, L.-P.; Martínez, T. J. TeraChem: A graphical processing unit-accelerated electronic structure package for large-scale ab initio molecular dynamics. *WIREs Comput. Mol. Sci.* **2021**, *11*, No. e1494.

(16) Giannozzi, P.; et al. QUANTUM ESPRESSO: a modular and open-source software project for quantum simulations of materials. *J. Phys.: Condens. Matter* **2009**, *21*, 395502.

(17) Giannozzi, P.; et al. Advanced capabilities for materials modelling with Quantum ESPRESSO. *J. Phys.: Condens. Matter* **2017**, *29*, 465901.

(18) Giannozzi, P.; Baseggio, O.; Bonfà, P.; Brunato, D.; Car, R.; Carnimeo, I.; Cavazzoni, C.; de Gironcoli, S.; Delugas, P.; Ferrari Ruffino, F.; Ferretti, A.; Marzari, N.; Timrov, I.; Urru, A.; Baroni, S. Quantum ESPRESSO toward the exascale. *J. Chem. Phys.* **2020**, *152*, 154105.

(19) Pederson, R.; Kozlowski, J.; Song, R.; Beall, J.; Ganahl, M.; Hauru, M.; Lewis, A. G. M.; Yao, Y.; Mallick, S. B.; Blum, V.; Vidal, G. Large Scale Quantum Chemistry with Tensor Processing Units. *J. Chem. Theory Comput.* **2023**, *19*, 25−32.

(20) Čížek, J. On the Correlation Problem in Atomic and Molecular Systems. Calculation of Wavefunction Components in Ursell-Type Expansion Using Quantum-Field Theoretical Methods. *J. Chem. Phys.* **1966**, *45*, 4256−4266.

(21) Bartlett, R. J. Many-Body Perturbation Theory and Coupled Cluster Theory for Electron Correlation in Molecules. *Annu. Rev. Phys. Chem.* **1981**, *32*, 359−401.

(22) Bartlett, R. J.; Musiał, M. Coupled-cluster theory in quantum chemistry. *Rev. Mod. Phys.* **2007**, *79*, 291.

(23) Shavitt, I.; Bartlett, R. J. *Many-Body Methods in Chemistry and Physics: MBPT and Coupled-Cluster Theory; Cambridge Molecular Science*; Cambridge University Press, 2009. DOI: 10.1017/CBO9780511596834.

(24) Bartlett, R. J. Perspective on Coupled-cluster Theory. The evolution toward simplicity in quantum chemistry. *Phys. Chem. Chem. Phys.* **2024**, *26*, 8013−8037.
(25) Lyakh, D. I.; Musiał, M.; Lotrich, V. F.; Bartlett, R. J. Multireference Nature of Chemistry: The Coupled-Cluster View. *Chem. Rev.* **2012**, *112*, 182−243.
(26) Evangelista, F. A. Perspective: Multireference coupled cluster theories of dynamical electron correlation. *J. Chem. Phys.* **2018**, *149*, 030901.
(27) Booth, G. H.; Thom, A. J. W.; Alavi, A. Fermion Monte Carlo without fixed nodes: A game of life, death, and annihilation in Slater determinant space. *J. Chem. Phys.* **2009**, *131*, 054106.
(28) Spencer, J. S.; Blunt, N. S.; Foulkes, W. M. The sign problem and population dynamics in the full configuration interaction quantum Monte Carlo method. *J. Chem. Phys.* **2012**, *136*, 054110.
(29) Shepherd, J. J.; Booth, G. H.; Alavi, A. Investigation of the full configuration interaction quantum Monte Carlo method using homogeneous electron gas models. *J. Chem. Phys.* **2012**, *136*, 244101.
(30) Booth, G. H.; Grüneis, A.; Kresse, G.; Alavi, A. Towards an exact description of electronic wavefunctions in real solids. *Nature* **2013**, *493*, 365−370.
(31) Zhang, S.; Krakauer, H. Quantum Monte Carlo Method using Phase-Free Random Walks with Slater Determinants. *Phys. Rev. Lett.* **2003**, *90*, 136401.
(32) Zhang, S. Auxiliary-field quantum Monte Carlo for correlated electron systems. *Emergent Phenomena in Correlated Matter*; Forschungezentrum Jülich, 2013; pp 15.1−15.26.
(33) Lee, J.; Pham, H. Q.; Reichman, D. R. Twenty Years of Auxiliary-Field Quantum Monte Carlo in Quantum Chemistry: An Overview and Assessment on Main Group Chemistry and Bond-Breaking. *J. Chem. Theory Comput.* **2022**, *18*, 7024−7042.
(34) Huron, B.; Malrieu, J. P.; Rancurel, P. Iterative perturbation calculations of ground and excited state energies from multiconfigurational zeroth-order wavefunctions. *J. Chem. Phys.* **1973**, *58*, 5745−5759.
(35) Evangelisti, S.; Daudey, J.-P.; Malrieu, J.-P. Convergence of an improved CIPSI algorithm. *Chem. Phys.* **1983**, *75*, 91−102.
(36) Holmes, A. A.; Tubman, N. M.; Umrigar, C. J. Heat-Bath Configuration Interaction: An Efficient Selected Configuration Interaction Algorithm Inspired by Heat-Bath Sampling. *J. Chem. Theory Comput.* **2016**, *12*, 3674−3680.
(37) Smith, J. E. T.; Mussard, B.; Holmes, A. A.; Sharma, S. Cheap and Near Exact CASSCF with Large Active Spaces. *J. Chem. Theory Comput.* **2017**, *13*, 5468−5478.
(38) Liu, W.; Hoffmann, M. R. iCI: Iterative CI toward full CI. *J. Chem. Theory Comput.* **2016**, *12*, 1169−1178.
(39) Zhang, N.; Liu, W.; Hoffmann, M. R. Iterative Configuration Interaction with Selection. *J. Chem. Theory Comput.* **2020**, *16*, 2296−2316.
(40) Zimmerman, P. M. Strong correlation in incremental full configuration interaction. *J. Chem. Phys.* **2017**, *146*, 224104.
(41) Zimmerman, P. M. Incremental full configuration interaction. *J. Chem. Phys.* **2017**, *146*, 104102.
(42) Eriksen, J. J.; Lipparini, F.; Gauss, J. Virtual Orbital Many-Body Expansions: A Possible Route towards the Full Configuration Interaction Limit. *J. Phys. Chem. Lett.* **2017**, *8*, 4633−4639.
(43) Sharma, S.; Holmes, A. A.; Jeanmairet, G.; Alavi, A.; Umrigar, C. J. Semistochastic Heat-Bath Configuration Interaction Method: Selected Configuration Interaction with Semistochastic Perturbation Theory. *J. Chem. Theory Comput.* **2017**, *13*, 1595−1604.
(44) Schriber, J. B.; Evangelista, F. A. Communication: An adaptive configuration interaction approach for strongly correlated electrons with tunable accuracy. *J. Chem. Phys.* **2016**, *144*, 161106.
(45) Tubman, N. M.; Lee, J.; Takeshita, T. Y.; Head-Gordon, M.; Whaley, K. B. A deterministic alternative to the full configuration interaction quantum Monte Carlo method. *J. Chem. Phys.* **2016**, *145*, 044112.
(46) Affleck, I.; Kennedy, T.; Lieb, E. H.; Tasaki, H. Rigorous results on valence-bond ground states in antiferromagnets. *Phys. Rev. Lett.* **1987**, *59*, 799−802.
(47) Fannes, M.; Nachtergaele, B.; Werner, R. F. Finitely correlated states on quantum spin chains. *Communications in Mathematical Physics* **1992**, *144*, 443−490.
(48) White, S. R. Density matrix formulation for quantum renormalization groups. *Phys. Rev. Lett.* **1992**, *69*, 2863−2866.
(49) White, S. R. Density-matrix algorithms for quantum renormalization groups. *Phys. Rev. B* **1993**, *48*, 10345−10356.
(50) Nishino, T. Density Matrix Renormalization Group Method for 2D Classical Models. *J. Phys. Soc. Jpn.* **1995**, *64*, 3598−3601.
(51) Östlund, S.; Rommer, S. Thermodynamic Limit of Density Matrix Renormalization. *Phys. Rev. Lett.* **1995**, *75*, 3537−3540.
(52) Rommer, S.; Östlund, S. Class of ansatz wave functions for one-dimensional spin systems and their relation to the density matrix renormalization group. *Phys. Rev. B* **1997**, *55*, 2164.
(53) White, S. R.; Martin, R. L. Ab initio quantum chemistry using the density matrix renormalization group. *J. Chem. Phys.* **1999**, *110*, 4127−4130.
(54) Schollwöck, U. The density-matrix renormalization group. *Rev. Mod. Phys.* **2005**, *77*, 259−315.
(55) Legeza, Ö.; Noack, R.; Sólyom, J.; Tincani, L. In *Computational Many-Particle Physics*; Fehske, H., Schneider, R., Weiße, A., Eds.; *Lecture Notes in Physics*, Vol. *739*; Springer: Berlin, Heidelberg, 2008; pp 653−664. DOI: 10.1007/978-3-540-74686-7_24.
(56) Chan, G. K.-L.; Zgid, D. In *The Density Matrix Renormalization Group in Quantum Chemistry*; Wheeler, R. A., Ed.; Annual Reports in Computational Chemistry, Vol. *5*; Elsevier, 2009; Chapter 7, pp 149−162.
(57) Schollwöck, U. The density-matrix renormalization group in the age of matrix product states. *Annals of Physics* **2011**, *326* (1), 96−192.
(58) Chan, G. K.-L.; Sharma, S. The Density Matrix Renormalization Group in Quantum Chemistry. *Annu. Rev. Phys. Chem.* **2011**, *62*, 465−481.
(59) Szalay, Sz.; Pfeffer, M.; Murg, V.; Barcza, G.; Verstraete, F.; Schneider, R.; Legeza, Ö. Tensor product methods and entanglement optimization for ab initio quantum chemistry. *Int. J. Quantum Chem.* **2015**, *115*, 1342−1391.
(60) Orús, R. Tensor networks for complex quantum systems. *Nature Reviews Physics* **2019**, *1*, 538−550.
(61) Chan, G. K.-L.; Keselman, A.; Nakatani, N.; Li, Z.; White, S. R. Matrix Product Operators, Matrix Product States, and ab initio Density Matrix Renormalization Group algorithms. *J. Chem. Phys.* **2016**, *145*, 014102.
(62) Baiardi, A.; Reiher, M. The density matrix renormalization group in chemistry and molecular physics: Recent developments and new challenges. *J. Chem. Phys.* **2020**, *152*, 040903.
(63) Reiher, M.; Wiebe, N.; Svore, K. M.; Wecker, D.; Troyer, M. Elucidating reaction mechanisms on quantum computers. *Proc. Natl. Acad. Sci. U. S. A.* **2017**, *114*, 7555−7560.
(64) Li, Z.; Li, J.; Dattani, N. S.; Umrigar, C. J.; Chan, G. K.-L. The electronic complexity of the ground-state of the FeMo cofactor of nitrogenase as relevant to quantum simulations. *J. Chem. Phys.* **2019**, *150*, 024302.
(65) Goings, J. J.; White, A.; Lee, J.; Tautermann, C. S.; Degroote, M.; Gidney, C.; Shiozaki, T.; Babbush, R.; Rubin, N. C. Reliably assessing the electronic structure of cytochrome P450 on today's classical computers and tomorrow's quantum computers. *Proc. Natl. Acad. Sci. U. S. A.* **2022**, *119*, e2203533119.
(66) Weser, O.; Freitag, L.; Guther, K.; Alavi, A.; Li Manni, G. Chemical insights into the electronic structure of Fe(II) porphyrin using FCIQMC, DMRG, and generalized active spaces. *Int. J. Quantum Chem.* **2021**, *121*, No. e26454.
(67) Sono, M.; Roach, M. P.; Coulter, E. D.; Dawson, J. H. Heme-Containing Oxygenases. *Chem. Rev.* **1996**, *96*, 2841−2888.
(68) Schöneboom, J. C.; Lin, H.; Reuter, N.; Thiel, W.; Cohen, S.; Ogliaro, F.; Shaik, S. The Elusive Oxidant Species of Cytochrome

P450 Enzymes: Characterization by Combined Quantum Mechanical/Molecular Mechanical (QM/MM) Calculations. *J. Am. Chem. Soc.* **2002**, *124*, 8142−8151.
(69) Meunier, B.; de Visser, S. P.; Shaik, S. Mechanism of Oxidation Reactions Catalyzed by Cytochrome P450 Enzymes. *Chem. Rev.* **2004**, *104*, 3947−3980.
(70) Phung, Q. M.; Feldt, M.; Harvey, J. N.; Pierloot, K. Toward Highly Accurate Spin State Energetics in First-Row Transition Metal Complexes: A Combined CASPT2/CC Approach. *J. Chem. Theory Comput.* **2018**, *14*, 2446−2455.
(71) Li Manni, G.; Alavi, A. Understanding the Mechanism Stabilizing Intermediate Spin States in Fe(II)-Porphyrin. *J. Phys. Chem. A* **2018**, *122*, 4935−4947.
(72) Li Manni, G.; Smart, S. D.; Alavi, A. Combining the Complete Active Space Self-Consistent Field Method and the Full Configuration Interaction Quantum Monte Carlo within a Super-CI Framework, with Application to Challenging Metal-Porphyrins. *J. Chem. Theory Comput.* **2016**, *12*, 1245−1258.
(73) Li Manni, G.; Kats, D.; Tew, D. P.; Alavi, A. Role of Valence and Semicore Electron Correlation on Spin Gaps in Fe(II)-Porphyrins. *J. Chem. Theory Comput.* **2019**, *15*, 1492−1497.
(74) Hasan, M. Z.; Kane, C. L. Colloquium: Topological insulators. *Rev. Mod. Phys.* **2010**, *82*, 3045−3067.
(75) Yan, S.; Huse, D. A.; White, S. R. Spin-Liquid Ground State of the S = 1/2 Kagome Heisenberg Antiferromagnet. *Science* **2011**, *332*, 1173−1176.
(76) Kitaev, A. Y. Unpaired Majorana fermions in quantum wires. *Physics-Uspekhi* **2001**, *44*, 131.
(77) Alicea, J. New directions in the pursuit of Majorana fermions in solid state systems. *Rep. Prog. Phys.* **2012**, *75*, 076501.
(78) Kitaev, A. Fault-tolerant quantum computation by anyons. *Annals of Physics* **2003**, *303*, 2−30.
(79) Varma, C. M. Colloquium: Linear in temperature resistivity and associated mysteries including high temperature superconductivity. *Rev. Mod. Phys.* **2020**, *92*, 031001.
(80) Bednorz, J. G.; Müller, K. A. Possible highTc superconductivity in the Ba-La-Cu-O system. *Zeitschrift für Physik B Condensed Matter* **1986**, *64*, 189−193.
(81) Yankowitz, M.; Chen, S.; Polshyn, H.; Zhang, Y.; Watanabe, K.; Taniguchi, T.; Graf, D.; Young, A. F.; Dean, C. R. Tuning superconductivity in twisted bilayer graphene. *Science* **2019**, *363*, 1059−1064.
(82) Chan, G. K.-L.; Head-Gordon, M. Highly correlated calculations with a polynomial cost algorithm: A study of the density matrix renormalization group. *J. Chem. Phys.* **2002**, *116*, 4462−4476.
(83) Legeza, Ö.; Röder, J.; Hess, B. A. Controlling the accuracy of the density-matrix renormalization-group method: The dynamical block state selection approach. *Phys. Rev. B* **2003**, *67*, 125114.
(84) Vidal, G. Class of Quantum Many-Body States That Can Be Efficiently Simulated. *Phys. Rev. Lett.* **2008**, *101*, 110501.
(85) Verstraete, F.; Cirac, J. I. Renormalization algorithms for Quantum-Many Body Systems in two and higher dimensions. *arXiv Preprint (Condensed Matter, Strongly Correlated Electrons)*, 2004. arXiv:cond-mat/0407066. https://arxiv.org/abs/cond-mat/0407066.
(86) Eisert, J.; Cramer, M.; Plenio, M. B. Colloquium: Area laws for the entanglement entropy. *Rev. Mod. Phys.* **2010**, *82*, 277−306.
(87) Vidal, G.; Latorre, J. I.; Rico, E.; Kitaev, A. Entanglement in Quantum Critical Phenomena. *Phys. Rev. Lett.* **2003**, *90*, 227902.
(88) Krumnow, C.; Veis, L.; Legeza, Ö.; Eisert, J. Fermionic Orbital Optimization in Tensor Network States. *Phys. Rev. Lett.* **2016**, *117*, 210402.
(89) Friesecke, G.; Werner, M. A.; Kapás, K.; Menczer, A.; Legeza, Ö. Global fermionic mode optimization via swap gates. *arXiv Preprint (Condensed Matter, Strongly Correlated Electrons)*, 2024. arXiv:2406.03449. https://arxiv.org/abs/2406.03449.
(90) Menczer, A.; Kapás, K.; Werner, M. A.; Legeza, Ö. Two-dimensional quantum lattice models via mode optimized hybrid CPU-GPU density matrix renormalization group method. *Phys. Rev. B* **2024**, *109*, 195148.
(91) Gunst, K.; Verstraete, F.; Wouters, S.; Legeza, Ö.; Van Neck, D. T3NS: Three-Legged Tree Tensor Network States. *J. Chem. Theory Comput.* **2018**, *14*, 2026−2033.
(92) Gunst, K.; Verstraete, F.; Van Neck, D. Three-Legged Tree Tensor Networks with SU(2) and Molecular Point Group Symmetry. *J. Chem. Theory Comput.* **2019**, *15*, 2996−3007.
(93) Cheng, Y.; Xie, Z.; Ma, H. Post-Density Matrix Renormalization Group Methods for Describing Dynamic Electron Correlation with Large Active Spaces. *J. Phys. Chem. Lett.* **2022**, *13*, 904−915.
(94) Hager, G.; Jeckelmann, E.; Fehske, H.; Wellein, G. Parallelization strategies for density matrix renormalization group algorithms on shared-memory systems. *J. Comput. Phys.* **2004**, *194*, 795−808.
(95) Stoudenmire, E. M.; White, S. R. Real-space parallel density matrix renormalization group. *Phys. Rev. B* **2013**, *87*, 155137.
(96) Nemes, C.; Barcza, G.; Nagy, Z.; Legeza, Ö.; Szolgay, P. The density matrix renormalization group algorithm on kilo-processor architectures: Implementation and trade-offs. *Comput. Phys. Commun.* **2014**, *185*, 1570−1581.
(97) Ganahl, M.; Milsted, A.; Leichenauer, S.; Hidary, J.; Vidal, G. TensorNetwork on TensorFlow: Entanglement Renormalization for quantum critical lattice models. *arXiv Preprint (Physics, Computational Physics)*, 2019. arxiv:1906.1203. https://arxiv.org/abs/1906.12030.
(98) Milsted, A.; Ganahl, M.; Leichenauer, S.; Hidary, J.; Vidal, G. TensorNetwork on TensorFlow: A spin chain application using tree tensor networks. *arXiv Preprint (Condensed Matter, Strongly Correlated Electrons)*, 2019. arxiv:1905.01331. https://arxiv.org/abs/1905.01331.
(99) Brabec, J.; Brandejs, J.; Kowalski, K.; Xantheas, S.; Legeza, Ö.; Veis, L. Massively parallel quantum chemical density matrix renormalization group method. *J. Comput. Chem.* **2021**, *42*, 534−544.
(100) Zhai, H.; Chan, G. K.-L. Low communication high performance ab initio density matrix renormalization group algorithms. *J. Chem. Phys.* **2021**, *154*, 224116.
(101) Gray, J.; Kourtis, S. Hyper-optimized tensor network contraction. *Quantum* **2021**, *5*, 410.
(102) Unfried, J.; Hauschild, J.; Pollmann, F. Fast time evolution of matrix product states using the QR decomposition. *Phys. Rev. B* **2023**, *107*, 155133.
(103) Ganahl, M.; Beall, J.; Hauru, M.; Lewis, A. G.; Wojno, T.; Yoo, J. H.; Zou, Y.; Vidal, G. Density Matrix Renormalization Group with Tensor Processing Units. *PRX Quantum* **2023**, *4*, 010317.
(104) Menczer, A.; Legeza, Ö. Massively Parallel Tensor Network State Algorithms on Hybrid CPU-GPU Based Architectures. *arXiv Prepint (Quantum Physics)*, 2023. arXiv:2305.05581. https://arxiv.org/abs/2305.05581.
(105) Menczer, A.; Legeza, Ö. Boosting the effective performance of massively parallel tensor network state algorithms on hybrid CPU-GPU based architectures via non-Abelian symmetries. *arXiv Preprint (Physics, Computational Physics)*, 2023. arXiv:2309.16724. https://arxiv.org/abs/2309.16724.
(106) Xiang, C.; Jia, W.; Fang, W.-H.; Li, Z. A distributed multi-GPU ab initio density matrix renormalization group algorithm with applications to the P-cluster of nitrogenase. *J. Chem. Theory Comput.* **2024**, *20*, 775−786.
(107) NVIDIA. *NVIDIA A100 Tensor Core GPU Architecture*, 2023. https://images.nvidia.com/aem-dam/en-zz/Solutions/data-center/nvidia-ampere-architecture-whitepaper.pdf.
(108) Menczer, A.; Legeza, Ö. *Petaflops Density Matrix Renormalization Group Method*, unpublished. 2023.
(109) Verstraete, F.; Nishino, T.; Schollwöck, U.; Bañuls, M. C.; Chan, G. K.; Stoudenmire, M. E. Density matrix renormalization group, 30 years on. *Nat. Rev. Phys.* **2023**, *5*, 273−276.
(110) Noack, R. M.; Manmana, S. R. Diagonalization- and Numerical Renormalization-Group-Based Methods for Interacting Quantum Systems. *AIP Conf. Proc.* **2005**, *789*, 93−163.
(111) Chan, G. K.-L.; Dorando, J. J.; Ghosh, D.; Hachmann, J.; Neuscamman, E.; Wang, H.; Yanai, T. In Frontiers in Quantum Systems in Chemistry and Physics; Wilson, S., Grout, P. J., Maruani,

https://doi.org/10.1021/acs.jctc.4c00903
J. Chem. Theory Comput. 2024, 20, 8397−8404

J., Delgado-Barrio, G., Piecuch, P., Eds.; *Progress in Theoretical Chemistry and Physics*; Springer: The Netherlands, 2008; Vol. *18*.
(112) Orús, R. A practical introduction to tensor networks: Matrix product states and projected entangled pair states. *Annals of Physics* **2014**, *349*, 117−158.
(113) Verstraete, F.; Murg, V.; Cirac, J. Matrix product states, projected entangled pair states, and variational renormalization group methods for quantum spin systems. *Adv. Phys.* **2008**, *57*, 143−224.
(114) Cirac, J. I.; Pérez-García, D.; Schuch, N.; Verstraete, F. Matrix product states and projected entangled pair states: Concepts, symmetries, theorems. *Rev. Mod. Phys.* **2021**, *93*, 045003.
(115) NVIDIA. NVIDIA DGX H100 TENSOR CORE GPU, 2023.https://resources.nvidia.com/en-us-dgx-systems/ai-enterprise-dgx.
(116) Chan, G. K.-L.; Kállay, M.; Gauss, J. State-of-the-art density matrix renormalization group and coupled cluster theory studies of the nitrogen binding curve. *J. Chem. Phys.* **2004**, *121*, 6110−6116.
(117) Reiher, M.; Wiebe, N.; Svore, K. M.; Wecker, D.; Troyer, M. Elucidating reaction mechanisms on quantum computers. *Proc. Natl. Acad. Sci. U. S. A.* **2017**, *114*, 7555−7560.
(118) Li, Z.; Li, J.; Dattani, N. S.; Umrigar, C. J.; Chan, G. K.-L. The electronic complexity of the ground-state of the FeMo cofactor of nitrogenase as relevant to quantum simulations. *J. Chem. Phys.* **2019**, *150*, 024302.
(119) Host refers to CPU where data are generated and device stands for the GPUs. Therefore, host-to-device (H2D) refers to data transfer from RAM to VRAM, while D2H from VRAM to RAM.
(120) NVIDIA. NVIDIA DGX GH200, . https://resources.nvidia.com/en-us-dgx-systems/nvidia-dgx-gh200-datasheet-web-us.
(121) AMD. AMD INSTINCT MI300A APU. https://www.amd.com/content/dam/amd/en/documents/instinct-tech-docs/data-sheets/amd-instinct-mi300a-data-sheet.pdf.
(122) Lynch, T.; Price, A. The effect of cytochrome P450 metabolism on drug response, interactions, and adverse effects. *Am. Fam. Physician* **2007**, *76*, 391−396.
(123) Zhao, M.; Ma, J.; Li, M.; Zhang, Y.; Jiang, B.; Zhao, X.; Huai, C.; Shen, L.; Zhang, N.; He, L.; Qin, S. Cytochrome P450 Enzymes and Drug Metabolism in Humans. *Int. J. Mol. Sci.* **2021**, *22*, 12808.
(124) Rask, A.; Zimmerman, P. M. The many-body electronic interactions of Fe (II)−porphyrin. *J. Chem. Phys.* **2022**, *156*, 094110.
(125) Veis, L.; Antalik, A.; Brabec, J.; Neese, F.; Legeza, Ö.; Pittner, J. Coupled Cluster Method with Single and Double Excitations Tailored by Matrix Product State Wave Functions. *J. Phys. Chem. Lett.* **2016**, *7*, 4072−4078.
(126) Barcza, G.; Werner, M. A.; Zaránd, G.; Pershin, A.; Benedek, Z.; Legeza, Ö.; Szilvási, T. Toward Large-Scale Restricted Active Space Calculations Inspired by the Schmidt Decomposition. *J. Phys. Chem. A* **2022**, *126*, 9709−9718.
(127) Friesecke, G.; Barcza, G.; Legeza, Ö. Predicting the FCI energy of large systems to chemical accuracy from restricted active space density matrix renormalization group calculations. *J. Chem. Theory Comput.* **2024**, *20*, 87−102.
(128) Zgid, D.; Nooijen, M. The density matrix renormalization group self-consistent field method: Orbital optimization with the density matrix renormalization group method in the active space. *J. Chem. Phys.* **2008**, *128*, 144116.
(129) Legeza, O.; Sólyom, J. Optimizing the density-matrix renormalization group method using quantum information entropy. *Phys. Rev. B* **2003**, *68*, 195116.
(130) Faulstich, F. M.; Mate, M.; Laestadius, A.; Csirik, M. A.; Veis, L.; Antalik, A.; Brabec, J.; Schneider, R.; Pittner, J.; Kvaal, S.; Legeza, Ö. Numerical and Theoretical Aspects of the DMRG-TCC Method Exemplified by the Nitrogen Dimer. *J. Chem. Theory Comput.* **2019**, *15*, 2206−2220.
(131) Bensberg, M.; Mörchen, M.; Stein, C. J.; Unsleber, J. P.; Weymuth, T.; Reiher, M. *qcscine/autocas*, Release 2.3.0; 2024.
(132) White, S. R. Density-matrix algorithms for quantum renormalization groups. *Phys. Rev. B* **1993**, *48*, 10345.
(133) Bellonzi, N.; et al. Feasibility of accelerating homogeneous catalyst discovery with fault-tolerant quantum computers. *arXiv Preprint (Quantum Physics)*, 2024. arXiv:2406.06335. https://arxiv.org/abs/2406.06335.
(134) Zhou, Y.; Stoudenmire, E. M.; Waintal, X. What Limits the Simulation of Quantum Computers? *Phys. Rev. X* **2020**, *10*, 041038.
(135) Chen, J.; Stoudenmire, E.; White, S. R. Quantum Fourier Transform Has Small Entanglement. *PRX Quantum* **2023**, *4*, 040318.
(136) Stoudenmire, E. M.; Waintal, X. Grover's Algorithm Offers No Quantum Advantage. *arXiv Preprint (Quantum Physics)*, 2023. arXiv:2303.11317. https://arxiv.org/abs/2303.11317.
(137) Pan, F.; Chen, K.; Zhang, P. Solving the Sampling Problem of the Sycamore Quantum Circuits. *Phys. Rev. Lett.* **2022**, *129*, 090502.
(138) Lee, S.; Lee, J.; Zhai, H.; Tong, Y.; Dalzell, A. M.; Kumar, A.; Helms, P.; Gray, J.; Cui, Z.-H.; Liu, W.; et al. Evaluating the evidence for exponential quantum advantage in ground-state quantum chemistry. *Nat. Commun.* **2023**, *14*, 1952.
(139) Rudolph, M. S.; Chen, J.; Miller, J.; Acharya, A.; Perdomo-Ortiz, A. Decomposition of Matrix Product States into Shallow Quantum Circuits. *arXiv Preprint (Quantum Physics)*, 2022. arXiv:2209.00595. https://arxiv.org/abs/2209.00595.
(140) Rudolph, M. S.; Miller, J.; Motlagh, D.; Chen, J.; Acharya, A.; Perdomo-Ortiz, A. Synergistic pretraining of parametrized quantum circuits via tensor networks. *Nat. Commun.* **2023**, *14*, 8367.
(141) Vidal, G. Efficient classical simulation of slightly entangled quantum computations. *Phys. Rev. Lett.* **2003**, *91*, 147902.
(142) Vidal, G.; Latorre, J. I.; Rico, E.; Kitaev, A. Entanglement in quantum critical phenomena. *Physical review letters* **2003**, *90*, 227902.
(143) Daley, A. J.; Kollath, C.; Schollwöck, U.; Vidal, G. Time-dependent density-matrix renormalization-group using adaptive effective Hilbert spaces. *Journal of Statistical Mechanics: Theory and Experiment* **2004**, *2004*, P04005.
(144) Haegeman, J.; Lubich, C.; Oseledets, I.; Vandereycken, B.; Verstraete, F. Unifying time evolution and optimization with matrix product states. *Phys. Rev. B* **2016**, *94*, 165116.
(145) Ferris, A. J.; Poulin, D. Tensor Networks and Quantum Error Correction. *Phys. Rev. Lett.* **2014**, *113*, 030501.
(146) Brandejs, J.; Saue, T.; Visscher, L.; Gomes, A.; Bientinesi, P. *CECAM Workshop on Tensor Contraction Library Standardization*. https://tensor.sciencesconf.org/.

https://doi.org/10.1021/acs.jctc.4c00903
J. Chem. Theory Comput. 2024, 20, 8397−8404